

1N-31  
371977

# Hybrid Damping System for an Electronic Equipment Mounting Shelf

Final Report  
for  
NASA - Ames University Consortium  
Joint Research Interchange

February 1, 1995 - January 31, 1997

## COLLABORATORS:

David Voracek  
Structural Dynamic Section  
NASA - Ames Research Center  
Dryden Flight Research Facility

Faysal A. Kolkailah, Ph.D., P.E.  
Principal Investigator  
Professor of Aeronautical Engineering  
California Polytechnic State University

## Assistant Investigators

J.R. Cavalli  
Eltahry Elghandour

To: CASI

Funds for the support of this study have been allocated by the NASA - Ames Research Center,  
Moffett Field, California under Interchange No. NCC2-5110

## **Abstract**

### **Hybrid Damping System for an Electronic Mounting Shelf**

Faysal A. Kolkailah, Ph.D., P.E.

The objective of this study was to design and construct a vibration control system for an electronic equipment shelf to be evaluated in the NASA Dryden FTF-II. The vibration control system was a hybrid system which included passive and active damping techniques. Passive damping was fabricated into the equipment shelf using ScotchDamp™ damping film and aluminum constraining layers. Active damping was achieved using a two channel active control circuit employing QuickPack™ sensors and actuators. Preliminary Chirp test results indicated passive damping smoothed the frequency response while active damping reduced amplitudes of the frequency response for most frequencies below 500Hz.

## **Acknowledgments**

I would like to thank NASA Dryden Flight Research Facility and NASA Ames Research Center for their sponsorship of this study. In addition, I would like to take this opportunity to express my gratitude to Dave Voracek and Mike Kehoe for their technical and administrative assistance during the course of this research effort and many others in the past. Last, but certainly not least, I would like to thank the assistants and undergraduate students involved with this project.

### **Assistants:**

**J.R. Cavalli  
Eltahry Elghandour**

### **Undergraduate Students:**

**Alex Silva  
Karen Soria  
Veronica Soria**

## Table of Contents

NOMENCLATURE.....	1
Subscripts.....	1
Acronyms.....	1
INTRODUCTION.....	2
Project Objectives.....	3
PASSIVE DAMPING.....	4
FINITE ELEMENT MODEL.....	5
TEST EQUIPMENT.....	8
ACTIVE DAMPING SYSTEM.....	10
Control Unit.....	10
Power Amplifier.....	13
QuickPack™ Actuators.....	14
Power Distribution System.....	14
Tuning the Active Damping System.....	15
DYNAMIC TESTING OF SHELF.....	16
Chirp Tests.....	16
Sinusoidal Tests.....	17
RESULTS AND DISCUSSION.....	18
Passive Damping.....	18
Active Damping.....	19
Active Damping Resolution.....	19
CONCLUSIONS.....	20
RECOMMENDATIONS.....	21
REFERENCES.....	22

## List of Tables

Table 1 - COSMOSM finite element model parameters.....	5
Table 2 - Instrumentation and equipment.....	8
Table 3 - Active damping system components.....	10
Table 4 - Network Analyzer data acquisition parameters.....	16
Table 5 - Chirp test configurations.....	17

## List of Figures

<b>Figure 1 - The Flight Test Facility FTF-II mounted on the lower fuselage of the F-15B. ....</b>	<b>2</b>
<b>Figure 2 - Passive damping lay-up for equipment shelf. ....</b>	<b>4</b>
<b>Figure 3 - Mode shapes of the equipment shelf and 5lb electronic box computed using COSMOSM. ....</b>	<b>6</b>
<b>- Mode shapes of the equipment shelf and 5lb electronic box computed using COSMOSM (continued). ....</b>	<b>7</b>
<b>Figure 4 - Experimental test equipment and active damping components. ....</b>	<b>9</b>
<b>Figure 5 - Active control analog circuit. ....</b>	<b>11</b>
<b>Figure 6 - Active control circuit board layout. ....</b>	<b>12</b>
<b>Figure 7 - Control unit. ....</b>	<b>13</b>
<b>Figure 8 - Power amplifier for piezoelectric actuators. ....</b>	<b>13</b>
<b>Figure 9 - QuickPack™ actuator layout. ....</b>	<b>14</b>
<b>Figure 10 - Distribution block circuit board layout. ....</b>	<b>15</b>
<b>Figure 11 - Block diagram of equipment setup for Chirp tests. ....</b>	<b>16</b>
<b>Figure 12 - Frequency response of Chirp excitation. ....</b>	<b>17</b>
<b>Figure 13 - Frequency Response of electronic mounting shelves using Chirp excitation. ....</b>	<b>18</b>

## NOMENCLATURE

l	length
t	thickness
w	width
C	capacity
F	farad
U	displacement
R	resistance or rotation
$\Omega$	ohms

## Subscripts

1, 2, ...	layers or modes
x	x direction
y	y direction
z	z direction

## Acronyms

ACSL	Aerospace Composites and Structures Laboratory
ACX	Active Control Experts
AGC	Automatic Gain Control
DAQ	Data Acquisition
FG	Function Generator
FE	Finite Element
FRF	Frequency Response Functions
FTF	Flight Test Facility
IC	Integrated Circuit
PZT	Piezoelectric Zirconate Titanate
QP	QuickPack <sup>™</sup>
VI	Virtual Instrument

## INTRODUCTION

Vibrations transmitted through an aircraft due to aerodynamics, propulsion systems, and mechanical systems reduce the performance and life expectancy of instrument components. There are two main techniques presently being pursued in vibration control which can be categorized as passive or active damping methods. In the past, passive methods such as special shock absorbing mounting brackets have been used to help reduce problems caused by vibration. More recently, damping films in conjunction with constraining layers are being manufactured as a part of the structure itself. Active damping methods utilizing piezoelectric ceramics are being considered to enhance equipment mounting platforms by further damping vibrations using phase cancellation. Signals produced by vibrations are detected with sensors, phase shifted using circuitry, and then re-introduced to the structure with actuators to cancel undesirable vibrations. This technology is commonly referred to as Smart Structures and can be better understood using the analogy of nerve, brain, and muscle interactions. Sensors, acting as nerves, sense the vibration of structure. A control system, acting as the brain, reacts to cancel vibration. And actuators, acting as muscles, provide a reaction force to damp vibration.

NASA Dryden Flight Research Engineer's have developed a second generation Flight Test Fixture, FTF-II, to be used as a generic test bed for research. The FTF-II shown in Figure 1

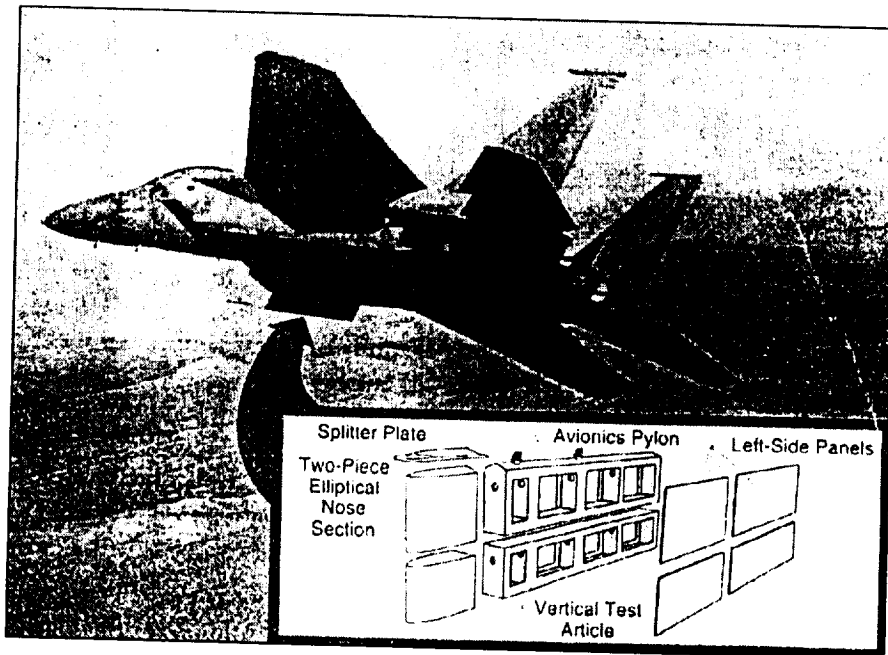


**Figure 1 - The Flight Test Facility FTF-II mounted on the lower fuselage of the F-15B.**

is a low aspect ratio, fin-like structure mounted on the centerline of the lower fuselage of an F-15B aircraft. The fixture is 107" long, 32" high, and 8" wide with an elliptical nose section and blunt trailing edge. Built primarily of carbon/epoxy material, the fixture consists of a pylon with removable side panels, nose section, and a vertical test article. Modular configuration makes it possible to modify the FTF-II to satisfy a variety of flight test requirements. The upper section of the FTF-II is a permanent structure that houses avionics, permanent research instrumentation systems, and other support equipment common to most flight experiments. The lower section of the FTF-II is the vertical test article, which, is removable and can be replaced by vertical test articles of other aerodynamic shapes. Normally, instrumentation specific to a research experiment are installed in the vertical test article. [Ref. 1]

### *Project Objectives*

In a joint research interchange between California Polytechnic State University and NASA entitled ***Optimizing Piezoelectric Sensors/Actuators for Vibration Damping***, an active damping system incorporating surface mounted piezoelectric ceramic sensors and actuators and an analog control circuit was developed to damp out the first bending mode of a model sailplane aluminum wing. Employing a similar multi-channel version of the active control system, the objective of this study was to design and construct a vibration control system for an electronic equipment shelf to be evaluated in the FTF-II. The hybrid vibration control system included passive and active damping technics. The following tasks were completed over a two year period.

- Modeled the passively damped equipment shelf mounted with a 5lb electronic box using COSMOSM finite element analysis program.
- Developed a two channel active damping system using piezoelectric sensors/actuators and analog circuits.
- Optimized and packaged active damping system into portable control unit for evaluation in the FTF-II.
- Conducted preliminary dynamic testing of the hybrid damping system of the equipment shelf.

The remaining task to complete is the evaluation of the hybrid damping system in the FTF-II.



## PASSIVE DAMPING PASSIVE DAMPING

As indicated in the **Introduction**, the hybrid damping system designed and constructed in this investigation included both passive and active techniques. The 19" x 6.5" x 0.149" passively damped electronic equipment shelf was fabricated from a larger 20" x 19" laminated plate which was manufactured by 3M Corporation and provided by NASA to Cal Poly for the purpose of this investigation. The plate was comprised of seven layers of aluminum and damping film as described here and shown in Figure 2.

- one layer: 100mil thick 5052 aluminum layer,
- three layers: 5mil thick viscoelastic layers,
- three layers: 10mil thick 1145 aluminum constraining layers

The viscoelastic layers were 3M Scotchdamp<sup>™</sup> damping film.

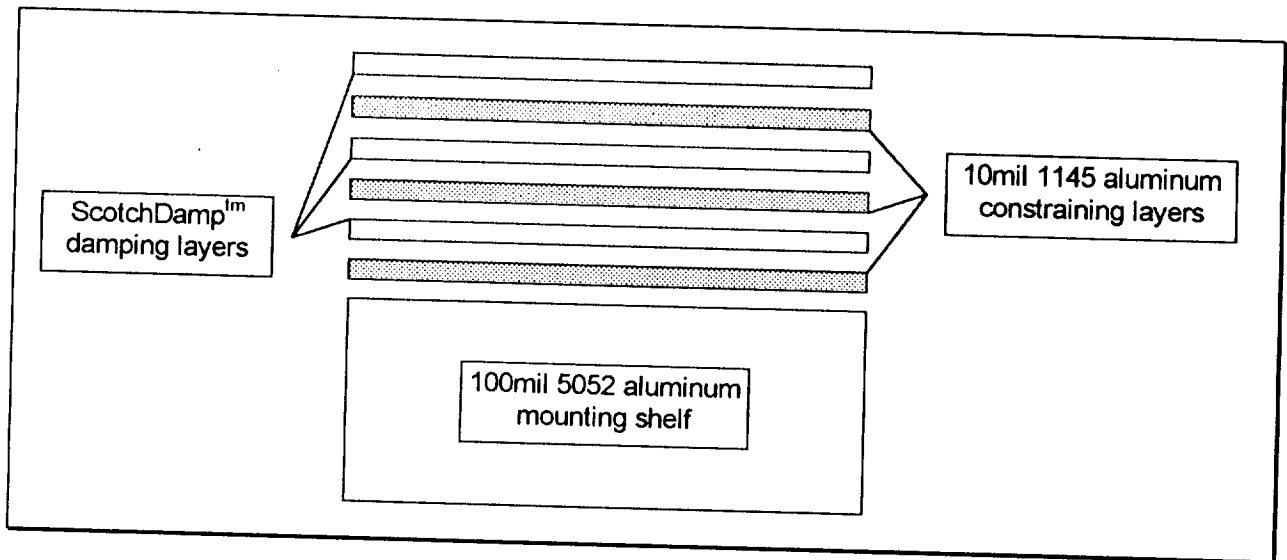


Figure 2 - Passive damping lay-up for equipment shelf.

## FINITE ELEMENT MODEL

The choice of actuator and sensor locations was an important issue in the design of the active damping system for the equipment shelf. Actuators needed to be placed at locations which optimized their damping effectiveness. This required determining regions of high average strain for targeted modes.

Finite element analysis of the equipment shelf mounted with a 5lb electronic box was performed using COSMOS/M version 1.75. The finite element model provided a prediction of the first eight mode shapes of the layered shelf and consisted of the parameters shown in Table 1.

<u>Mounting Shelf:</u>	
SHELL4L:	510 elements, 4-node
7 layers:	1 layer 6061_ Aluminum , $t_1 = 0.1"$ 3 layers DampFilm, $t_2 = t_4 = t_6 = 0.005"$ 3 layers Aluminum, $t_3 = t_5 = t_7 = 0.01"$
meshing:	surface mesh
B.C.'s:	double cantilever , $U_x = U_y = U_z = 0, R_x = R_y = R_z = 0$
<u>Electronic Box:</u>	
SOLID:	432 elements, 8 node
dimensions:	L = 3.86", W = 3.10", H = 4.00" STEEL with density adjustment.
meshing:	volume mesh
B.C.'s:	bottom surface nodes merged to top surface of shelf
<u>Analysis:</u>	
Subspace Iteration solution method; Lump mass matrix formulation	

**Table 1 - COSMOSM finite element model parameters.**

The use of SHELL4L elements allowed for the shelf to be modeled as a multiple layer thin shell. The selection of this element was based on the necessities to model multiple layers with several different materials and to model elements that had length to thickness aspect ratios between 2 and 4. The model included 1 layer of 100mil 6061 aluminum, 3 layers of 5mil damping film, and 3 layers of 10mil aluminum. The actual equipment shelf was constructed of 1145 and 5054 aluminum, however, the material properties of these two aluminum could not be located, therefore, 6061\_Aluminum and Aluminum contained in the COSMOSM material property library were substituted as best estimations for 5054 aluminum and 1145 aluminum, respectively. The damping film was modeled by creating a new material property for the COSMOSM library using best guest estimations of the Modulus of Elasticity and Modulus of Rigidity based on ScotchDamp<sup>™</sup> material property information provided by 3M Corporation. Density was calculated using mass and volume measured from damping film samples. The shelf was surface meshed with 510, 4-node, elements. Boundary conditions at the cantilever edges of the shelf were constrained in all directions, that is, displacements  $U_x = U_y = U_z = 0$  and rotations  $R_x = R_y = R_z = 0$ .

library with a high rigidity. The density property of steel was adjusted to create a 5lb box with the dimensions of 3.86" x 3.10" x 4.00".

The boundary conditions between the electronic box and shelf were joined by merging nodes on the bottom surface of the box and the top surface of the shelf within a proximity tolerance of 0.006". The solution was computed using subspace iteration method and neglected damping. Mode shapes and frequencies predicted by COSMOSM for the first 8 modes are shown in Figure 3a) - h).

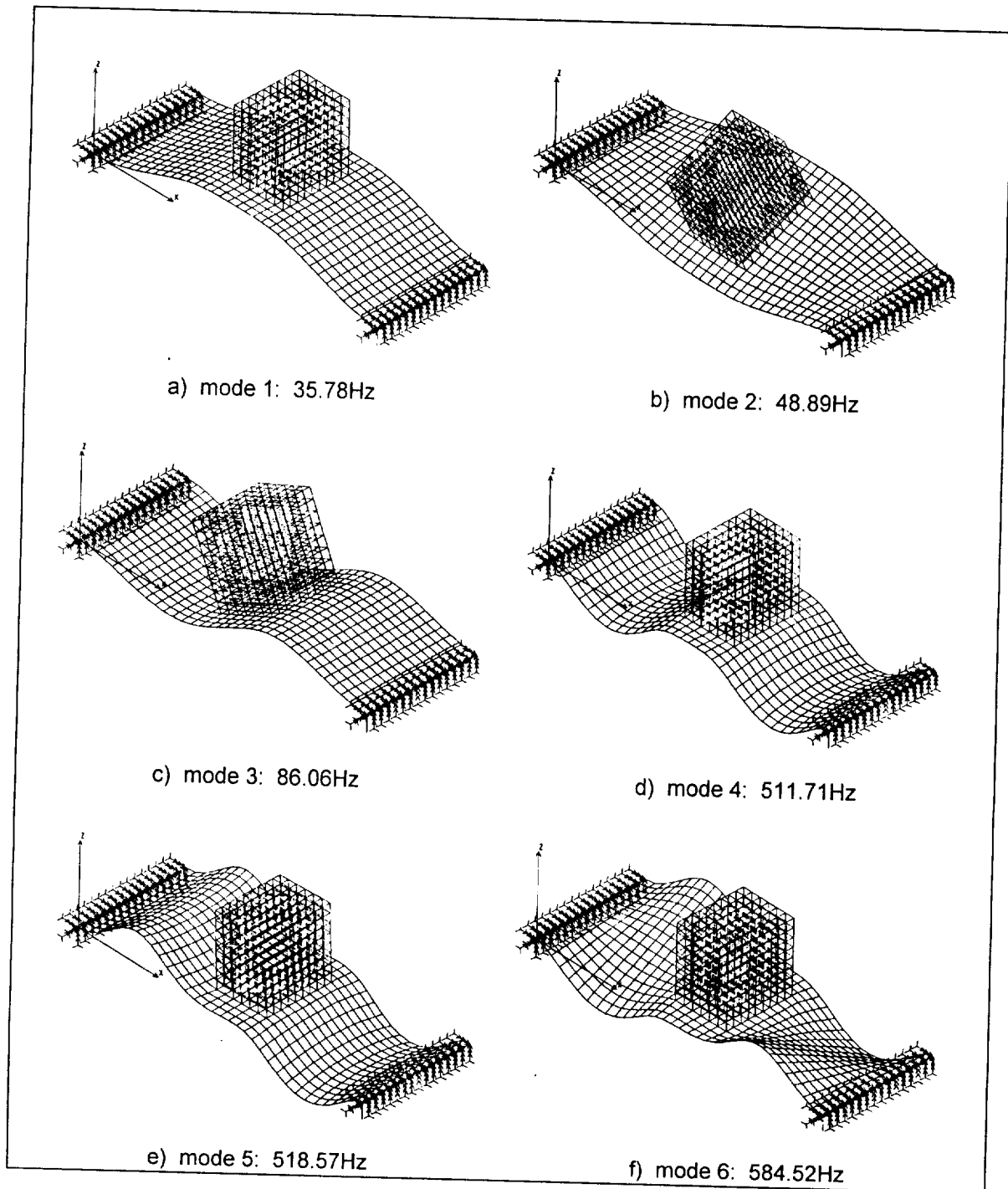
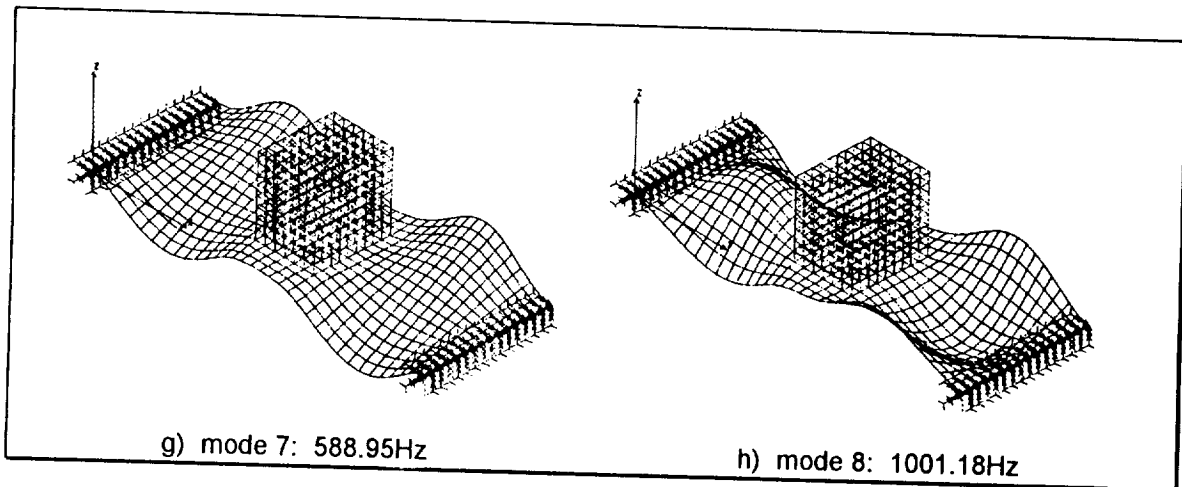


Figure 3 - Mode shapes of the equipment shelf and 5lb electronic box computed using COSMOSM.



**Figure 3 - Mode shapes of the equipment shelf and 5lb electronic box computed using COSMOSM (continued).**

As can be seen from Figure 3, except for the first few mode shapes, the node line patterns were complicated and intersected in vertical and horizontal directions. For this reason, it was decided to target the first and second bending modes, Figure 3a) and 3c), by placing piezoelectric sensors and actuators at outboard locations near the cantilever edges and at the inboard locations near the box edge.

## TEST EQUIPMENT

Table 2 below summarizes the equipment utilized in the investigation conducted at Cal Poly Aerospace Composites and Structures Laboratory, ACSL.

<u>item</u>	<u>make</u>	<u>model</u>	<u>specifications</u>
a) PC Computer	Weston	ø	486DX2 - 66MHz 16M RAM
a) Data Acquisition Card	National Instruments	AT-MIO-16F-5	16 channels
a) Network Analyzer	National Instruments	LabVIEW for Windows	Version 3.0
b) Connector Block	National Instruments	CB-100	100 connections
c) Function Generator	Hewlett-Packard	3311A	0Hz - 1MHz
d) Power Amplifier	MB Electronics	2250MB	ø
e) Shaker Pod	MB Electronics	ø	ø
f) Suspension Table	Cal Poly	ø	7074T aluminum Dim.: 21" x 21" x 0.25"
g) Box Frame	Cal Poly	ø	Inside Dim.: 19" x 12" x 7.75"
h) Oscilloscope	Tektron	T912	2 Channel
i) Oscilloscope	Tektron	2215	2 Channel
j) Signal Conditioner	Kistler	5122	4 Channel
Accelerometer	Kistler	8636B500	range: 500 g sensitivity: 10.01 mV/g
k) Voltmeter	B & K Tool Kit	2707	200mV - 1000V 0kHz - 200Hz 0W - 200MW 0A - 10A

**Table 2 - Instrumentation and equipment..**

The data acquisition system consisted of a 486DX2-66 Weston PC compatible computer with 16MB of RAM, a National Instruments AT-MIO-16F-5 Data Acquisition (DAQ) card, a CB-100 connector block, and LabVIEW for Windows Network Analyzer virtual instrument software.

Sinusoidal and Chirp excitation signals were generated by the HP function generator and Network Analyzer, respectively. Excitation signal gain was boosted through the power amplifier before entering the shaker pod. The electronic equipment shelf was mounted into a 19" x 12" x 7.75" box frame constructed of 0.75" maple wood sandwiched by two 1.5" wide, 0.25" thick 7074T aluminum frames. The box frame was secured to a 21" x 21" x 0.25" 7074T aluminum table and suspended at the four corners by two surgical tube bands. The suspension table was design to reduce vertical loading on the shaker pod created by the weight of the box frame. Two Tektronix oscilloscopes monitored input and output signals of the active damping system. An accelerometer and signal conditioner in conjunction with the DAQ system was used to take measurements at various locations on the shelf and box frame. Troubleshooting the active control circuit and accurately measuring frequencies during sinusoidal tests was accomplished

using the multipurpose voltmeter. Figure 4 shows the experimental test equipment, as well as, the active damping components discussed in the succeeding section.

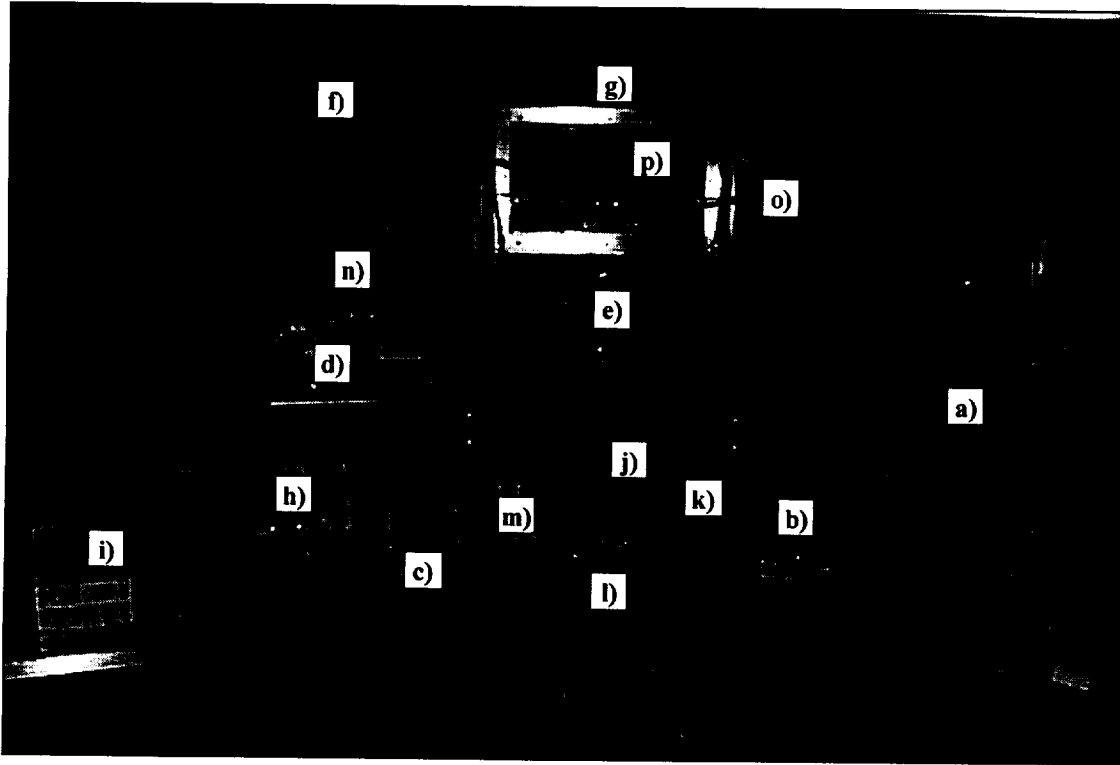


**Figure 4 - Experimental test equipment and active damping components.**

## ACTIVE DAMPING SYSTEM

The active damping system employed five basic components; a control unit, DC power supplies, a power amplifier, piezoelectric sensors and actuators, and a power distribution block and cables. A 5lb box filled with brass standards was used to simulate a piece of electronic hardware equipment. Table 3 summarizes the components of the active damping system shown in the Figure 4.

<u>item</u>	<u>make</u>	<u>model</u>	<u>specifications</u>
l) Control Unit	Cal Poly	PD2000	2 channel
m) Power Supply	Heathkit	IP-2718	0 - 20 volts DC three output
n) Power Amplifier	Kettering Systems	KC-2	2 channel Dim.:16.75"x10.75"x 3.5" weight: est. 15lbs ranges: $\pm 200$ volts $\pm 200$ mA power: 20 Wrms gain: 1x to 20x
QuickPack <sup>lm</sup> Actuators	ACX	QP20W	size: 2" x 1.5" x 0.03" weight: 0.28 oz piezo wafers: 2 1.81" x 1.31" x 0.01" range: $\pm 200$ volts
o) Power Distribution System	Cal Poly	PDB-1	two BNC inputs to four 16- pin outputs, four cables
p) Electronic Box	Cal Poly	$\phi$	5lbs brass standards

**Table 3 - Active damping system components.**

### *Control Unit*

The control unit housed a two channel analog control circuit based on the single channel analog circuit developed in ***Optimizing Piezoelectric Sensors/Actuators for Vibration Damping*** Ref.[2]. The working premise of the damping system was very simple. Given an input signal provided by a mechanical transducer (sensor), filter unwanted frequencies, phase shift, amplify, and return the signal to a set of mechanical transducers (actuators) which provide an appropriate reaction force to damp out targeted resonant frequencies of a structure.

Each channel of the control unit contained buffer, low pass filter, phase shifter, and gain circuit components as shown in Figure 5. The buffer circuit provided high impedance input and a DC offset adjustment of the sensor input signal. Piezoelectric sensors signals typically incurred a slight positive DC offset due to higher structural deflections in the downward gravitational direction. The buffer circuit was comprised of the LM301 and LM924 operational amplifiers. Two 180° phase shifters allowed phase adjustments of up to approximately 360° between input and output signals. Two 2nd order low-pass filters minimized potentiometer noise and high frequency noise from sensor signals before entering the pre-amplifier. Channels 1 and 2 were constructed with a low pass filter cut-off frequencies of 175Hz and 350Hz, respectively. One 14 pin LM348 (quad LM741) op-amp was used for the two phase shifters and two low-pass filters of each channel. Pre-gain amplification was achieved by a LM343 high performance inverting

amplifier. Positive and negative DC voltage regulators utilizing LM317 and LM337 chips, respectively, supplied  $\pm 12$  volts to all integrated circuit, IC, chips.

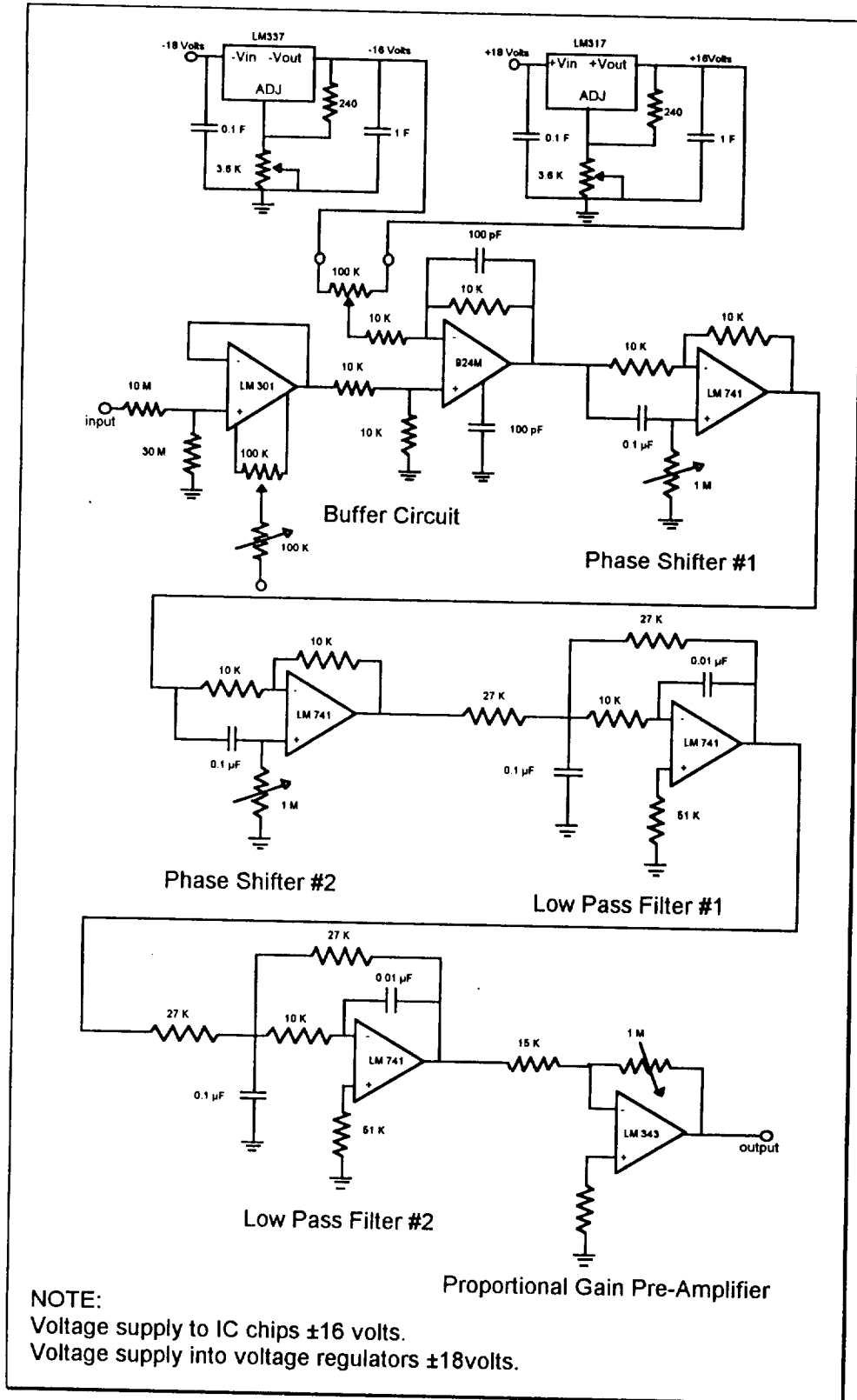


Figure 5 - Active control analog circuit..



The two channels of the control system were constructed and tested on a bread board and then transferred to a circuit board. The circuit layout shown in Figure 6 was etched into a

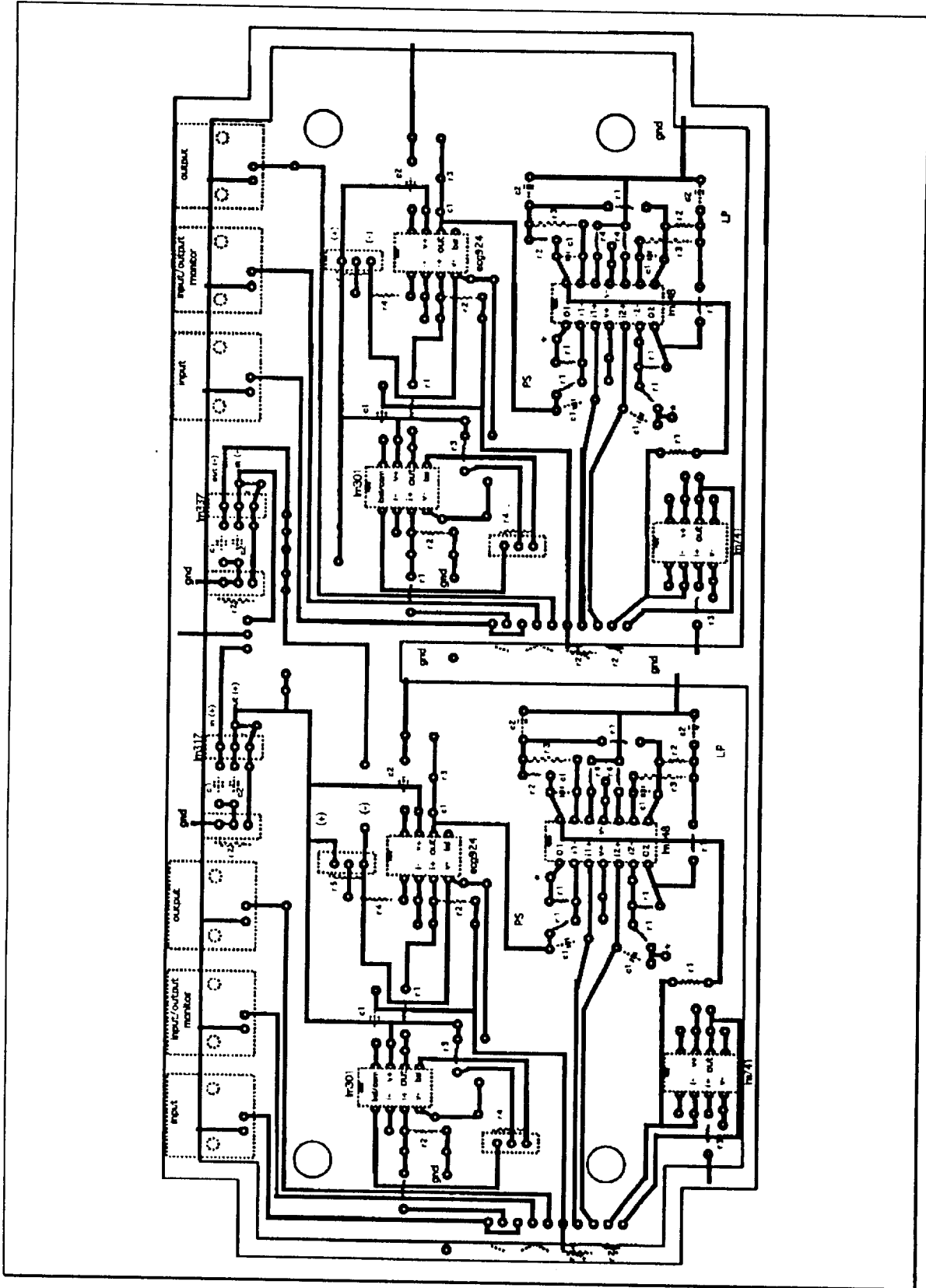


Figure 6 - Active control circuit board layout.

single sided copper clad board. Labels, shown as dotted lines, show locations of component parts and were not etched. All IC chips were mounted in socket seats. The outer border outline was common ground for all components.

The circuit board was sized to mount into the control unit shown in Figure 7. The control unit allowed for turn-knob adjustment of phase shift and gain, and turn-screw adjustment of the DC offset for each channel. In addition, each channel had a 3-way switch to allow monitoring of the input signal and output signals and a 2-way switch for on/off control of active damping. Six BNC connectors, 3 per channel, were used for input, output, and monitor signals. A voltage of  $\pm 18$ Volts to the control unit was provided by a Heathkit Tri-Power Supply via a 3-pin connector.

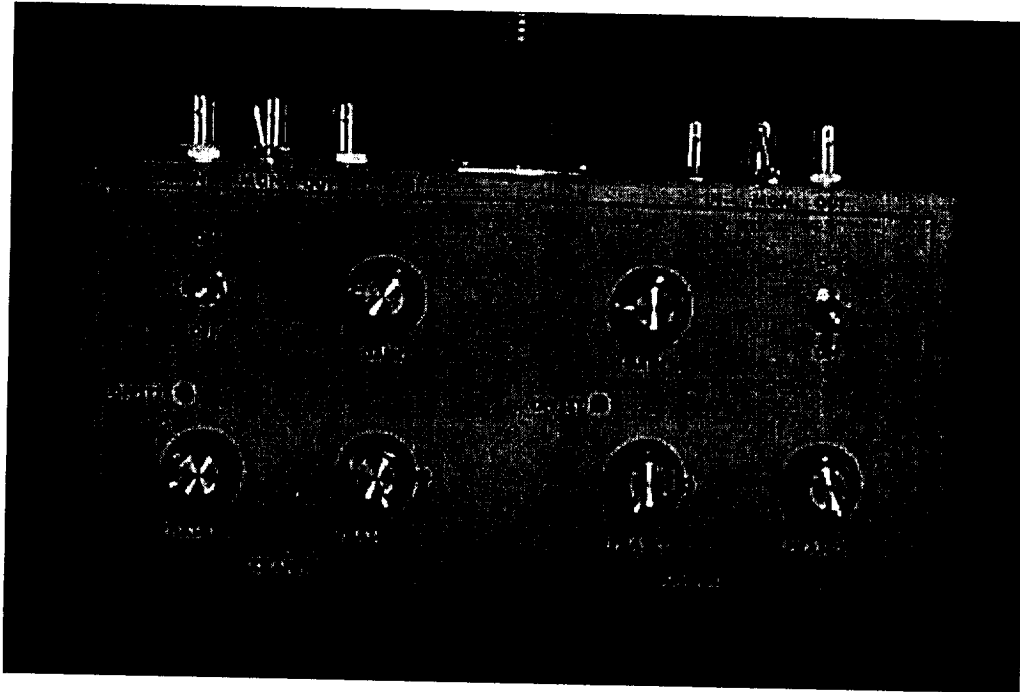


Figure 7 - Control unit.

### Power Amplifier

The KC-2 two channel power amplifier shown in Figure 8 was specifically designed and built to power piezoelectric actuators. The design was based on the single channel QuickPack<sup>™</sup> Power Amplifier manufactured by ACX. The amplifier could deliver up to 20 Watts,  $\pm 200$  Volts,

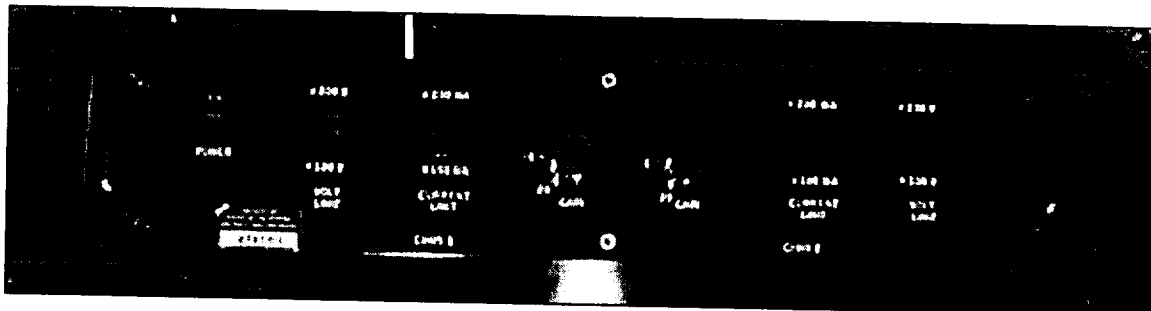


Figure 8 - Power amplifier for piezoelectric actuators.

and  $\pm 200$ mA per channel. In addition, it had selectable voltage and current limit protection and 1x to 20x continuous, adjustable gain for each channel. On the back panel BNC connectors were used for input and output signals. The dimensions of the rack-mount amplifier case was

16.75"x10.75"x3.5" and weighed approximately 15lbs. The design goal was not size and weight but, to insure maximum power could be delivered to all actuators.

### *QuickPack™ Actuators*

The piezoelectric sensors and actuators used in the investigation were QP20W QuickPack™, QP, Actuators purchased from ACX. As shown in Figure 9a), a total of sixteen, four columns of four, 2.0"x1.5"x0.03" actuators were secured to the bottom surface of the shelf using epoxy. For purpose of discussion, the center two columns of four actuators are referenced as the inboard QPs and the outer two columns of four actuators are referenced as the outboard QPs.

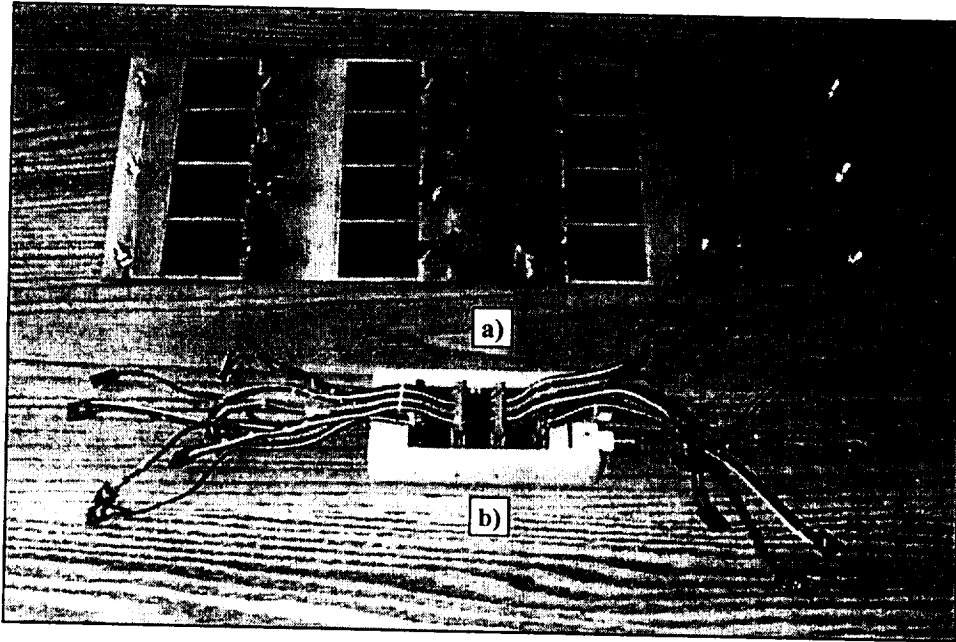


**Figure 9 - QuickPack™ actuator layout.**

Each QP contained two ceramic wafers measuring 1.81"x1.31"x0.010" weighing 0.28 oz., had an operating range of  $\pm 200$ Volts, and included a four pin male connector. Each unit was connected for extension-compression operation, leads 1 and 4 were grounds and leads 2 and 3 were given an applied voltage, and could be used as a sensor or actuator.

### *Power Distribution System*

The power distribution system, shown in Figure 9b) and consisting of a distribution block and cables, was constructed to provide reliable distribution of the two input signal to fifteen QPs, seven of which received channel 1, and eight of which received channel 2. To achieve this, a circuit board etched from single sided copper clad board routed two BNC inputs to four, 16-pin male connectors. The cables further subdivided the signal to four, 4-pin female connectors which plugged into the QP. One outboard QP (labeled "s" in Figure 9a) ) was used as sensors for both channels. This was possible because each QP contained two independent piezoelectric wafers.

The distribution block allowed for multiple channel and actuator hook-up combinations. The optimum configuration used the center two 16-pin connectors for the eight inboard QPs and the outer two 16-pin connectors for eight outboard QPs. The distribution block and cables worked very well. Figure 10 is a diagram of the circuit board layout used to create the distribution block. Labels, shown as dotted lines, show locations of connectors.

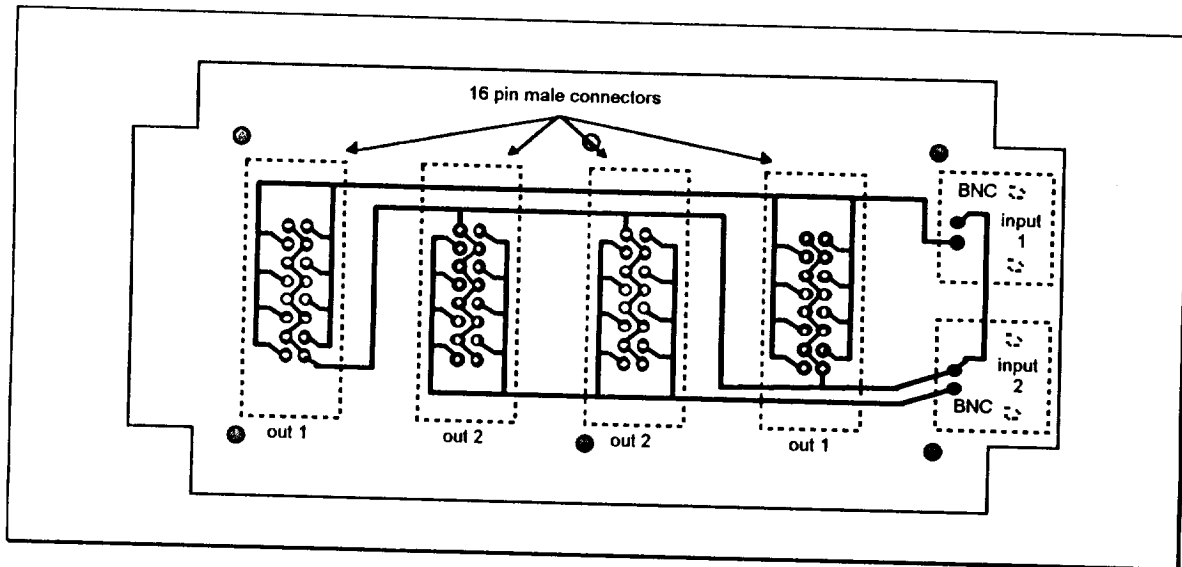


Figure 10 - Distribution block circuit board layout.

### *Tuning the Active Damping System* **Tuning the Active Damping**

Tuning each channel of the active damping circuit for maximum damping involved several steps and oscilloscopes for monitoring sensor and actuator signals of each channel. The procedure began by exciting the shelf at the first resonant mode using sinusoidal excitation. With the control unit off, phase shift and gain knobs turned full counter clockwise, and the power amplifier turned on with full gain, the control unit was switch on and the gain increased until the system began to become unstable, at which time the phase shifters were adjusted until stability was restored and a decrease in sensor signal observed. With the active system remaining on, the gain was once again increased until the system began to become unstable and the phase shift readjusted to stabilize the system. When phase shift adjustment could no longer stabilize the system, the gain was slightly decreased until stability returned. Maximum damping for a channel occurred when the sensor signal lead the actuator signal by approximately 90°.

## DYNAMIC TESTING OF SHELF DYNAMIC TESTING OF SHELF

### Chirp Tests

Figure 11 is a block diagram of the equipment setup for preliminary tests performed on the electronic equipment shelf. The Network Analyzer provided the Chirp excitation input signal to the shake table, as well as, time response data sampling using an accelerometer placed atop the 5lb box. In addition, the Network Analyzer calculated Frequency Response Functions, FRF's, from the time response data.

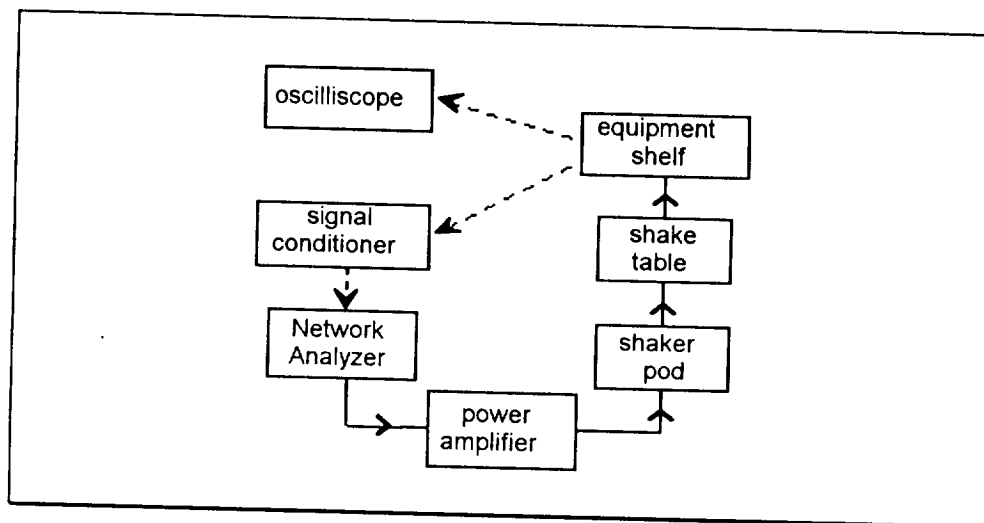


**Figure 11 - Block diagram of equipment setup for Chirp tests.**

The Network Analyzer parameters shown in Table 4 were determined the most suitable for Chirp excitation tests and were used to acquire results presented in this investigation.

Sample rate:	1024 samples/sec
Frame size:	1000 samples
Windowing:	none
Averaging:	1

**Table 4 - Network Analyzer data acquisition parameters.**

Based on the Nyquist Criteria, a sample rate of 1024 samples/sec provided a frequency bandwidth sweep of 0Hz-500Hz for the FRF's. A frame size of 1000 samples at 1024 samples/sec provided a sufficient corresponding frequency resolution of 0.9766Hz. No windowing or averaging was necessary. Figure 12 shows a frequency response function of a typical Chirp excitation. The data was acquired with an accelerometer placed on the shaker pod piston. More pertaining to Figure 12 will be presented in **Results and Discussion**. Excitation was implemented to produce a displacement in the vertical (z-axis) direction.

Chirp tests on the electronic equipment shelf were performed for the five configurations summarized in Table 5. All tests included a 5lb box mounted at the center of the equipment shelf. Configuration #1 was a solid 7074T aluminum shelf fabricated to dimensions typical of shelves currently being used to mount electronic equipment. Configurations #2 through #5 applied to the hybrid equipment shelf fabricated using multiple layers of aluminum and ScotchDamp™ film, and therefore, had passive damping built into the shelf. Configuration #2 included no active damping. Configuration #3, included single channel active damping provided by channel 1 and the 7 outboard actuators. Similarly, configuration #4 included single channel active damping provided by channel 2 and 8 inboard actuators. Configuration #5 included dual

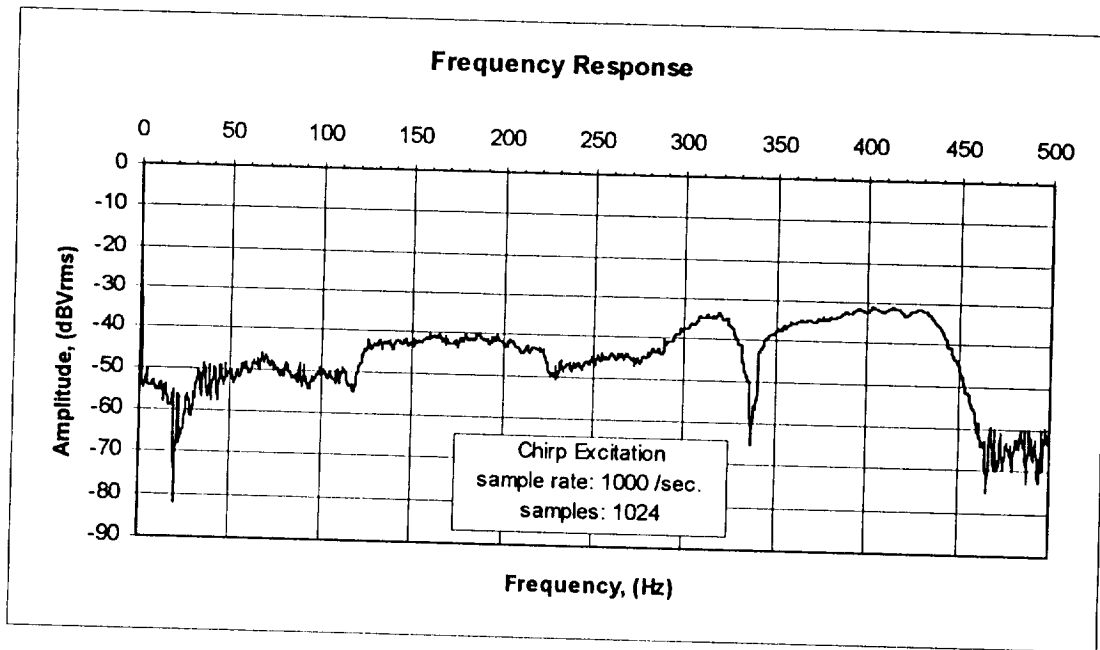


Figure 12 - Frequency response of Chirp excitation.

channel active damping provided by channels 1 and 2 and the 15 inboard and outboard actuators. These configurations were derived after testing multiple channel, sensor, and actuator combinations in an effort to maximize the active damping system.

<u>configuration</u>	<u>shelf</u>	<u>damping</u>
1	Solid	none
2	Hybrid	passive
3	Hybrid	passive active: channel 1, 8 actuators
4	Hybrid	passive active: channel 2, 8 actuators
5	Hybrid	passive active: channels 1 & 2, 16 actuators

Table 5 - Chirp test configurations.

#### *Sinusoidal Tests*

A second type of dynamic test conducted on the equipment shelf utilized sinusoidal excitation. The equipment setup was identical to that shown in Figure 11 except that a function generator provided a manually adjustable sinusoidal signal to the power amplifier.

Sinusoidal testing served two purposes. First, it was used to tune the shelf-box system to suspected resonant frequencies using visual and audio verification. And second, it was used to discriminate between frequency response peaks obtained by Chirp excitation test as resonant frequencies of the shelf-box system or as resonant frequencies of the shake-table-mounting-frame system. Except for the first bending mode of the equipment shelf, neither Chirp test or Sinusoidal test were capable of identifying mode shapes of suspected resonant frequencies.

## RESULTS AND DISCUSSION

As mentioned in the previous section, the preliminary results obtained for the solid aluminum shelf and the hybrid aluminum shelf were obtained using Chirp excitation. FRF's were calculated with time response data acquired using 1040 samples at a rate of 1000 samples/second. The configuration of the shelf included a center mounted 5lb box to simulate an electronic device. An accelerometer placed atop the 5lb box measured acceleration in the z direction.

Figure 13 below depicts the FRF's obtained for the five configurations of the solid and hybrid shelf discussed in Table 4. The black curve represents the FRF of the solid shelf.

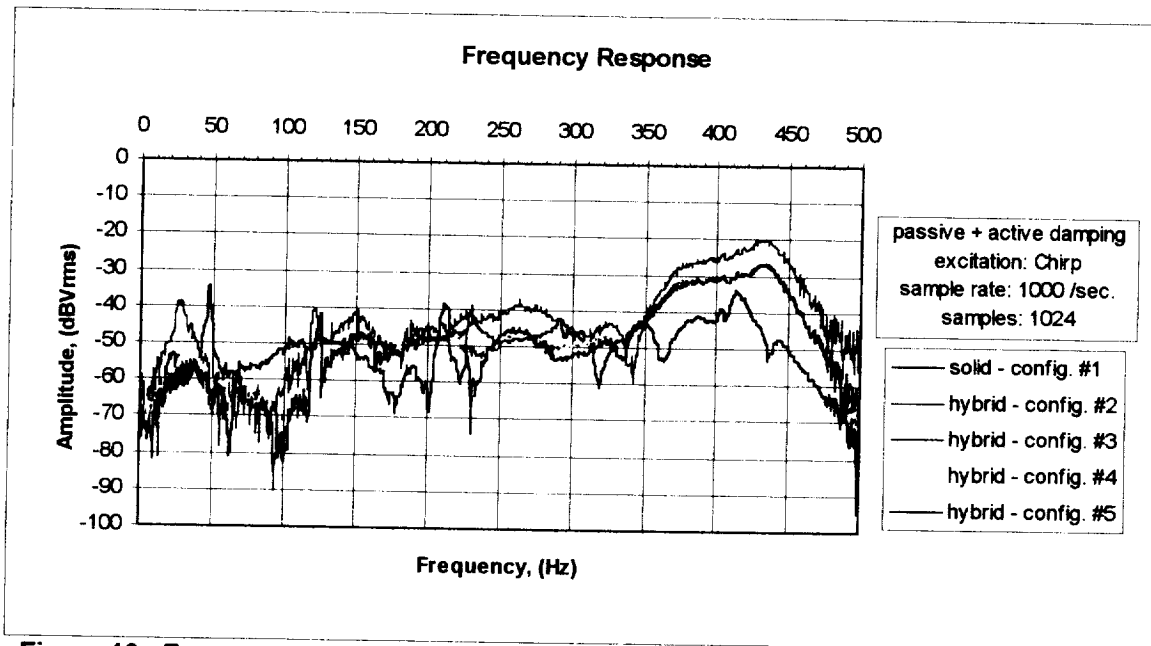


Figure 13 - Frequency Response of electronic mounting shelves using Chirp excitation.

The green FRF represents the hybrid shelf with no active damping. The red, yellow, and blue curves represent the FRF's of the hybrid shelf with channel 1 active damping, channel 2 active damping, and channel 1 & 2 active damping, respectively.

The fundamental resonant frequency was visually identified as the first bending mode shape and compared agreeably with the fundamental resonant frequency, 35.78Hz, and mode shape predicted by the finite element model. Efforts to create node traces of higher mode shapes using sugar were unsuccessful, and therefore, satisfactorily verifying higher mode shapes to those predicted by the finite element model was not possible.

### *Passive Damping*

Comparing the FRF's of configuration #1 and #2, the passive damping of the hybrid shelf was relatively more smooth, or less jagged, than the solid aluminum shelf. In addition, the hybrid shelf's fundamental resonant frequency of 28.3Hz was 19.6Hz lower than the fundamental resonant frequency of the solid shelf, 47.9Hz. This was primarily due to the fact that the solid shelf was approximately 100mils thicker than the hybrid shelf. The corresponding drop in amplitude from approximately -34dBVrms to -39dBVrms was attributed to the damping film and constraining layers.

### *Active Damping*

Comparing FRF's of the four configurations of the hybrid shelf indicated that active damping decreased response amplitudes of the majority of frequencies below 500Hz. In particular, the first bending mode, 30Hz, which the active control system was optimized to dampen, a decrease in the peak amplitude of 17dBVrms was observed. Somewhat of a surprise was the relatively similar performance of the active damping of channel 1 and channel 2 considering channel 1 used different actuator sets. The fact that the combined effectiveness of channels 1 and 2 was not the sum of the individual effectiveness was attributed to the decrease in sensor signal as the active damping system decreased the shelf deflections.

In an attempt to increase the sensor signal at low shelf deflections, an Automatic Gain Control, AGC, amplifier was constructed and tested. Unfortunately, existing designs were optimized to operate in the 300Hz to 120MHz range and performed unsatisfactorily at frequencies around 30Hz.

Response peaks common to both the solid and hybrid FRF's, such as the peaks at the frequencies of approximately 120Hz and 196Hz, were believed to be caused by resonant modes of the shake table and/or frame mounting fixture. The large rise of all the FRF's in the 350Hz to 450Hz range was believed to be primarily caused by the FRF of Chirp excitation (see Figure 12).

### *Active Damping Resolution*

An inherent problem with active damping higher modes with complex node line patterns was the difference in phase shift required by two adjacent actuators. Distribution of a single signal to multiple actuators worked well when the actuators required the same phase signal, such as the case for the first bending mode; however, the active damping system became unstable and impossible to tune when trying to tune for more complex modes. A method to correct the problem would have been to increase the active damping resolution. This would have required dedicating an active control circuit and power amplifier for each actuator on the shelf which would have allowed independent tuning of each active damping system.



## CONCLUSIONS

The objective of this investigation to design and construct a hybrid vibration damping system for an electronic mounting shelf was accomplished. In doing so, four of five tasks have been completed. A finite element model of the passively damped equipment shelf mounted with a 5lb electronic box was constructed. Results were used to develop a two channel active damping system using piezoelectric sensors/actuators and an analog circuit. The active damping system was optimized and housed into a portable control unit. Chirp test conducted on the hybrid damping system indicated that the use of passive damping films smoothed the FRF's while active damping diminished FRF amplitudes for most frequencies below 500Hz. It was also determined that active damping caused instability problems in the control circuit when attempts were made to target higher modes. Overall the hybrid damping system performed well but could be improved by increasing the active damping resolution. The final task left to complete is the evaluation of the hybrid damping system in the FTF-II.

## RECOMMENDATIONS

The following are two suggestions for improving the effectiveness of the active damping system:

The inherent problem of two adjacent actuators requiring different phase shifted signals for mode shapes with complex node patterns can be corrected by increasing the active damping resolution. One method for achieving this would be to dedicate an active control circuit for each actuator attached to the shelf. This would allow each active system to be independently tuned to its optimum damping effectiveness. The biggest obstacle in doing this is the cost of the power amplifiers. The biggest engineering obstacle is reducing the size and weight of each power amplifier.

In the existing active damping system the phase shift between sensor and actuator signals is dependent on frequency, therefore, each channel can only be tuned for one specific frequency. An improvement to this would be to design an analog circuit which can maintain a constant phase change tuning of  $90^\circ$  between the sensor and actuator signals independent of frequency.

## REFERENCES

1. "Flight-Test Fixture for Aerodynamic Research", NASA Tech Briefs, (September 1995).
2. Kolkailah, A. Faysal, "Optimizing Piezoelectric Sensors/Actuators for Vibration Damping", California Polytechnic State University, CA, (1993).
3. "Guide to Modern Piezoelectric Ceramics", Morgan Matroc Inc., Bedford, Ohio, (1991).
4. "Piezoelectric Technology: Data For Designers", Morgan Matroc Inc., Bedford, Ohio, (1991).
5. "Operational Amplifiers Databook", National Semiconductors Corporation, Santa Clara, CA, (1995 Edition).
6. "Linear Applications Handbook", National Semiconductors Corporation, Santa Clara, CA, (1994 Edition).
7. "General-Purpose/Linear ICs Data Handbook", Philips Semiconductors, Sunnyvale, CA, pgs:259-264, (1995 Edition).
8. Graf, F. Rudolf, "Encyclopedia of Electronic Circuits", TAB Books, Vol. 3, pg: 15, (1991).
9. Lindner, K. Douglas and Tabisz, A. Wojciech, "Miniaturized Power Converters For Smart Structure Applications", Virginia Tech, Blacksburg, VA 24061.
10. Starek, Ladislav, "Application of Smart Structures to the Vibration Suppression Problem", Slovak Technical University, nam. Slobody 17, 81231 Bratislava, Slovakia.
11. Ha, Sung K., Keilers, Charles, Chang, Fu-Kuo "Finite Element Analysis Composite Structures Containing Distributed Piezoceramic Sensors and Actuators" AIAA Journal , Vol. 30, No 3., (March 1992).
12. Liang, Chen; Sun, Fanping; Rogers A. Craig; "Coupled Electro-Mechanical analysis of Piezoelectric Ceramic Actuator-Driven Systems - Determination of the Actuator Power Consumption and System Energy Transfer", Virginia Polytechnic Institute and State University, Blacksburg, VA, (February 1993).